Reply to Anonymous Referee #2

We thank the reviewer for the careful reading of the manuscript and helpful comments. We have revised the manuscript following the suggestion, as described below.

Major comments:

1 Comment: While the authors provided many details in the methodology, there are still some missing important information. For example, BrC refractive index and DRE calculations are well explained, but AOD calculations are not mentioned in the methodology. Since the modeled AOD is discussed and compared with observations, the author should briefly describe the process of calculating AOD (e.g., Mie theory uses refractive indices as inputs?)

Response: As suggested, we have included Section "2.2 Aerosol radiative module" in Lines 98-123 in the main text:

"2.2 Aerosol radiative module

The aerosol radiative module developed by Li et al. (2011) has been incorporated into the WRF-Chem model to calculate the aerosol optical depth (AOD or τ_a), single scattering albedo (SSA or ω_a), and the asymmetry factor (g_a). In the aerosol module, aerosols are represented by a three-moment approach with a lognormal size distribution:

$$n(lnD) = \frac{N}{\sqrt{2\pi} ln\sigma_g} exp[-\frac{1}{2}(\frac{lnD-lnD_g}{ln\sigma_g})^2] \quad (1)$$

Where D is the particle diameter, N is the number distribution of all particles in the distribution, D_g is the geometric mean diameter, and σ_g is the geometric standard deviation. To calculate the aerosol optical properties, the aerosol spectrum is divided into 48 bins from 0.002 to 20.0 μm, with radius r_i. The aerosols are classified into four types: (1) internally mixed sulfate, nitrate, ammonium, hydrophilic organics and black carbon (BC), and water; (2) hydrophobic organics; (3) hydrophobic BC; and (4) other unidentified aerosols (generally dust-like aerosols). These four kinds of aerosols are assumed to be mixed externally. For the internally mixed aerosols, the complex refractive index at a certain wavelength (λ) is calculated based on the volume-weighted average of the individual refractive index. Given the particle size and complex refractive index, the extinction efficiency (Q_e), ω_a and g_a are calculated using the Mie theory at a certain wavelength (λ). The look-up tables of Q_e, ω_a and g_a are established according to particle sizes and refractive indices to avoid multiple Mie scattering calculation.

The aerosol optical parameters are interpolated linearly from the look-up tables with the calculated refractive index and particle size in the module. The τ_a at a certain λ in a given atmospheric layer k is determined by the summation over all types of aerosols and all bins:

$$\tau_a(\lambda,k) = \sum_{i=1}^{48}\sum_{j=1}^{4} Q_e\,(\lambda, r_i, j, k)\pi {r_i}^2 n(r_i, j, k)\Delta Z_k \quad (2)$$

where $n(r_i, j, k)$ is the number concentration of j-th kind of aerosols in the i-th bin. ΔZ_k is the depth of an atmospheric layer. The weighted-mean values of ω_a and g_a are then calculated by using D'Almeida et al., (1991):

$$\omega_a(\lambda,k) = \frac{\sum_{i=1}^{48}\sum_{j=1}^{4} Q_e(\lambda,r_i,j,k)\pi {r_i}^2 n(r_i,j,k)\omega_a(r_i,j,k)\Delta Z_k}{\sum_{i=1}^{48}\sum_{j=1}^{4} Q_e(\lambda,r_i,j,k)\pi {r_i}^2 n(r_i,j,k)\Delta Z_k} \quad (3)$$

$$g_a(\lambda,k) = \frac{\sum_{i=1}^{48}\sum_{j=1}^{4} Q_e(\lambda,r_i,j,k)\pi {r_i}^2 n(r_i,j,k)\omega_a(r_i,j,k)g_a(\lambda,r_i,j,k)\Delta Z_k}{\sum_{i=1}^{48}\sum_{j=1}^{4} Q_e(\lambda,r_i,j,k)\pi {r_i}^2 n(r_i,j,k)\omega_a(r_i,j,k)\Delta Z_k} \quad (4)$$

When the wavelength-dependent τ_a, ω_a, and g_a are calculated, they can be used in the Goddard shortwave module."

2 Comment: Any assumption made in the study needs either a reference or an explanation. There are multiple assumptions in your study that are not justified. For example, "In this work, a proportion of 10% of the total SOA is included as a part of BrC" or "The BrC in the model has an effective density of 1.2 g cm-3 for primary BrC and of 1.0 g cm-3 for secondary BrC".

Response: We have separated the aromatic SOA from the whole SOA produced from anthropogonic and biogenic sources in the model as suggested, setting the aromatic SOA as the secondary source of BrC. Additionally, since our study do not consider the dynamic variations of BrC absorption, we have added corresponding explanations. We have clarified in Lines 176-185 in main the text:

" SOA has also shown light absorption in the atmosphere (Lin et al., 2014). Laboratory experiments have revealed that most of the light-absorbing SOA is associated with aromatic SOA (Jacobson, 1999; Laskin et al., 2015; Li et al., 2020) and the absorption from biogenic SOA in the field has been found to be negligible (Washenfelder et al., 2015) . Therefore, here we assume aromatic derived SOA as secondary BrC in the model following previous studies (Jo et al., 2016; Wang et al., 2018).

Moreover, it is worth noting that both primary and SOA light absorption were shown to be dynamic, where BrC can be bleached when they undergo photodissociation (Forrister et al., 2015; Wong et al., 2019), or be darken by cloud and fog processing of aerosols (Moise et al., 2015; Lin et al., 2017; Cheng et al., 2020). These processes are not considered in this study yet.

More detailed parameterization of the chemical aging of BrC are needed in future BrC models. ”

We have added the references for the BrC effective density and clarified in Lines 134-135: “The BrC in the model has an effective density of 1.2 g cm^{-3} for primary BrC (Turpin and Lim, 2001) and of 1.0 g cm^{-3} for secondary BrC (Hurley et al., 2001).”

Minor comments:

1 Comment: Page 6, line 125: “RCC is responsible for about 45% of primary BrC emissions”. Is this percentage based on your calculations? Or from other studies or data? Please use proper citations or discuss the calculations further.

Response: We have re-established the proportions of BrC from various primary emission sources based on the “bottom-up” inventories. We have clarified in Lines 146-175 in the main text:

“ For the primary emission of BrC, previous BrC simulations have substituted it with a proportion of POA directly (Feng et al., 2013; Lin et al., 2014; Wang et al., 2014; Tuccella et al., 2020; Xu et al., 2024), derived it from the relationship between the burning efficiency and the observed aerosol light absorption (Jo et al., 2016; Zhu et al., 2021), or determined it through parameterization where BrC absorption is a function of the BC-to-OA emission ratio (Zhang et al., 2020). In the present work, we have calculated the primary BrC emissions based on the bottom-up OA emission inventory combined with reported annual BrC emissions from various primary sources, as shown in Table 1. Firstly, we collect the reported annual emissions of BrC from RCC, BB and FFs-TRA by using bottom-up inventory method. It should be noted that given the proximity of the study period (January 2014) to 2013, we use the emissions of BrC from RCC and BB in 2013 provided by Sun et al. (2017; 2021), which is 592 Gg and 712 Gg, respectively. The emissions of FFs-TRA derived BrC is 76Gg, which is calculated based on the value of 2017 (Wang et al., 2022) and scaled by a factor of 0.70 to reflect the change of annual civilian-owned motor vehicles. We assume that the spatial and seasonal variation of BrC is similar to OA. Then bottom-up emissions inventory induced monthly BrC emissions in the NCP in January 2014 is the annual BrC emissions multiplied by the ratio of OA emissions in the NCP *vs* China, and the ratio of OA emissions in January 2014 *vs* the whole year, resulting in a value of 65.5 Gg, 56.8 Gg and 4.4 Gg for RCC, BB and FFs-TRA, respectively. Finally, the proportion of the three primary emissions of BrC used in the model is 36.3%, 100.8% and

15.8%, respectively. Figure 2 shows the contributing regions and burdens of the three separated primary sources of BrC."

Table 1 The data for primary BrC emissions calculation

Primary sources of BrC	RCC	BB	FFs-TRA
Annual BrC emissions (Gg) in China	592.0[a]	712.0[b]	76.0[c]
Ratio of OA emissions in the NCP *vs* China[e]	57.7%	51.0%	69.4%
Ratio of OA emissions in January 2014 *vs* the whole year[e]	19.2%	14.0%	8.3%
Bottom-up emissions inventory induced monthly BrC emissions in the NCP in January	65.5	56.8[d]	4.4
Emissions in the NCP in January 2014[e]	180.2	56.4	27.9
BrC emissions ratio for primary sources used in the model	36.3%	100.8%	15.8%

[a] The BrC emissions from China's RCC in 2013 was reported by Sun et al., (2017) based on experiments involving seven coals were burned in four typical stoves as both chunk and briquette styles.
[b] The calculated BrC emissions from China's household biomass burning in 2013 reported by Sun et al., (2021) using 11 widely used biomass types in China burned in a typical stove.
[c] The estimated BrC emissions from vehicle exhaust in 2017 was 109 Gg reported by Wang et al., (Wang et al., 2022). In this study, the emissions of FFs-TRA derived BrC is 76.0 Gg with a yearly scale factor 0.70 which derived by the annual civilian-owned motor vehicles between 2014 and 2017.
[d] The value of BrC emissions in NCP in January 2014 is additionally added with OA emitted from the open-biomass burning (6 Gg) which is assumed to be entirely light-absorbing.
[e] These values were derived from the OA emission inventory described in Sec. 2.1

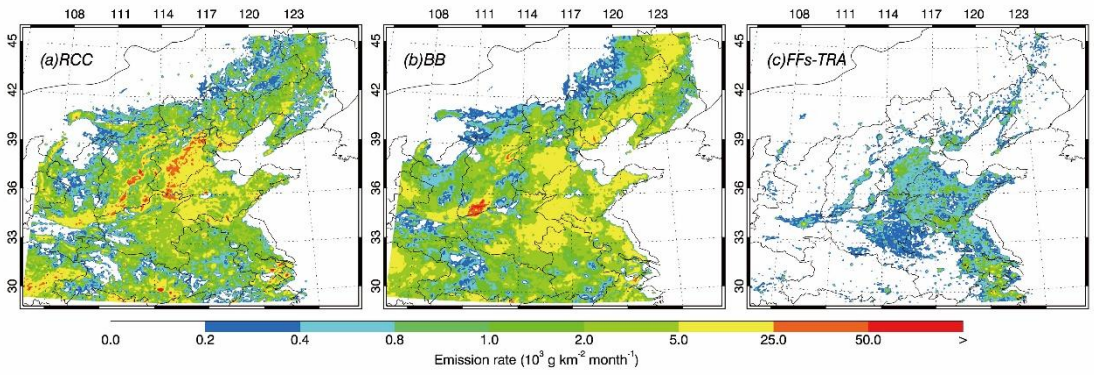

Figure 2 Monthly BrC emissions burdens in January 2014 in NCP from RCC, BB and FFs-TRA.

2 Comment: Page 7, line 148: Expand MAE when it appears for the first time. This applies to all other abbreviations used in the manuscript.

Response: We have explained MAE in Lines 195-196 and double checked other abbreviations in the main text and Supplement.

3 Comment: Page 9: Give more details on LGHAP and OMI satellites (e.g., horizontal resolution, local time overpass, etc.). Then discuss those further. For example, are you comparing model results at the satellite overpass time?

Response: We have added detailed descriptions of both the LGHAP in Lines 260-264 and OMI in Lines 272-274, respectively:
Lines 266-270: "This gap-free daily AOD dataset at 1 km resolution for 2000–2020 in China is generated by integrating multimodal data from satellites, numerical models, and in situ measurements. Data gaps in Moderate Resolution Imaging Spectroradiometer (MODIS) AOD are reconstructed through spatial pattern recognition and statistical knowledge transfer. Validation against Aerosol Robotic Network (AERONET) observations showed strong agreement, with an R of 0.91 and an RMSE of 0.21."
Lines 278-280: "OMI aboard NASA's Aura satellite offers global atmospheric measurements at a spatial resolution of 0.25°×0.25°, with Beijing's overpass occurring at approximately 13:45 local time. The average AOD440 from the model simulation at 14:00 local time shows generally agreement with the OMI retrieval."

4 Comment: Page 10, line 204: Change "hydroscopic" to "hygroscopic". Hygroscopic growth is the size increase of aerosols due to water vapor absorption.

Response: We have changed "hydroscopic" to "hygroscopic" in Line 284 in the main text.

5 Comment: Page 11, line 221: Change "ration" to "ratio".

Response: We have rephrased the sentence as "The underestimation might be partly caused by the overestimation of absorbing aerosols like BC or dust" in Lines 257-258 in the main text.

6 Comment: Page 13, line 259: Citation is needed for "Compared with the global mean ratio of BrC to BC which is 1.24".

Response: We have added the citation in Lines 326-328 in the main text.

7 Comment: Page 15, line 288: "the increased DRE_{TOA} induced by BrC which is usually considered as its scattering effect is up to an average of +0.37 W m-2 …". This sentence is confusing a little. The authors should clarify if they are talking about BrC's net radiative effect or just absorption. As mentioned in Page 15, line 285: "the BrC populations have a net cooling effect". So, the net BrC DRE could not increase OA DRE.

Response: We agree with the comment and have clarified in Line 404 in the main text: "the absorption of BrC increases the DRE_{TOA} of OA by 28.0% with an average of +0.40 W m^{-2} and a maximum of +1.83 W m^{-2}"

8 Comment: Figures 8 and 9: Panel letter C is missing.

Response: We have updated Figures 8 and 9.

9 Comment: Figure S1: Adding error bars to the time series would be helpful since the authors are demonstrating average concentrations over all the monitors in NCP.

Response: We have updated Figure S1 as suggested.

10 Comment: Figure S4: The units inside the charts (MB and RMSE) should be updated.

Response: We have updated the units (MB and RMSE) inside the charts as suggested.

In addition to the questions raised by the reviewer above, we have also reorganized the abstract of the manuscript and made some additional explanations in Lines 413-418 in the main text: "It should be noted that China has started to switch from coal to cleaner and more efficient energy such as natural gas or liquid petroleum gas in recent years. According to the latest report of National Bureau of Statistics of China, the total coal consumption for residential use is 55.5 Gg in 2022 (https://data.stats.gov.cn) with a 40.3% decrease compared to 2014. Therefore, our diagnosis of the sources of BrC and their radiative effects is specifically targeted at the winter season in 2014. Moreover, future simulations should strengthen the parameterization for the evolution of BrC, such as bleaching or darkening processes."

Furthermore, we have conducted additional sensitivity experiments on different *k* values.

NOBRC: All organic aerosols treated as purely scattering (no BrC absorption)；

LOW-BRC-ABS: BrC absorption with lower *k* values；

HI-BRC-ABS: BrC absorption with higher *k* values.

Comparisons of modeled and observed SSA across these experiments demonstrate that the HI-BRC-ABS configuration yields the closest agreement with observations. We have clarified in Lines 241-263 in the main test:

"SSA determines the strength of aerosols in absorbing solar radiation. Here we conduct three sensitivity experiments to evaluate the effect of BrC with different *k* values on the simulated aerosol absorption. The first experiment is the control simulation in which all organic aerosols are treated as purely scattering particles with no absorption contribution of BrC, which is referred to as NOBRC. The hi-absorption scenario (HI-BRC-ABS) and low-absorption scenario (LOW-BRC-ABS) characterize BrC light absorption by using the higher and lower imaginary refractive index derived from Section 2.3.2, respectively. Figure 3 shows the comparisons of simulated versus observed SSA at 440 nm (SSA440) at Sun-sky radiometer Observation NETwork (SONET) sites in Beijing, Songshan, Xi'an, Hefei, and Nanjing in January 2014. Due to the influence of clouds, the observational data from SONET are not continuous, resulting in a total of 237 valid data points are available for comparisons. Moreover, SSA retrieval typically have larger uncertainties at low AOD values (Dubovik et al., 2002). Therefore, we have excluded the SSA data when AOD is less than 0.5, which has 206 valid points in each case. We find that the inclusion of BrC in the model reduces the bias of simulated SSA. The HI-BRC-ABS case demonstrated a largest improvement with the correlation coefficient increasing to 0.54, making it the best simulation in the study. It suggests that stronger BrC absorption case, as prescribed in HI-BRC-ABS, better captures the aerosol optical properties observed in northern China during the winter. Consequently, The HI-BRC-ABS case can serve as the base simulation for further investigation of radiative effects of BrC in this study. Overall, the model tends to underestimate SSA_{440}. The underestimation might be partly caused by the overestimation of absorbing aerosols like BC or dust. Meanwhile, the uncertainties of the simulated SSA can be caused by other factors, such as mixing state of aerosols, particle shape, wavelength, and mass ration of non-black carbon to BC (Liu et al., 2017; Jeong et al., 2020)."

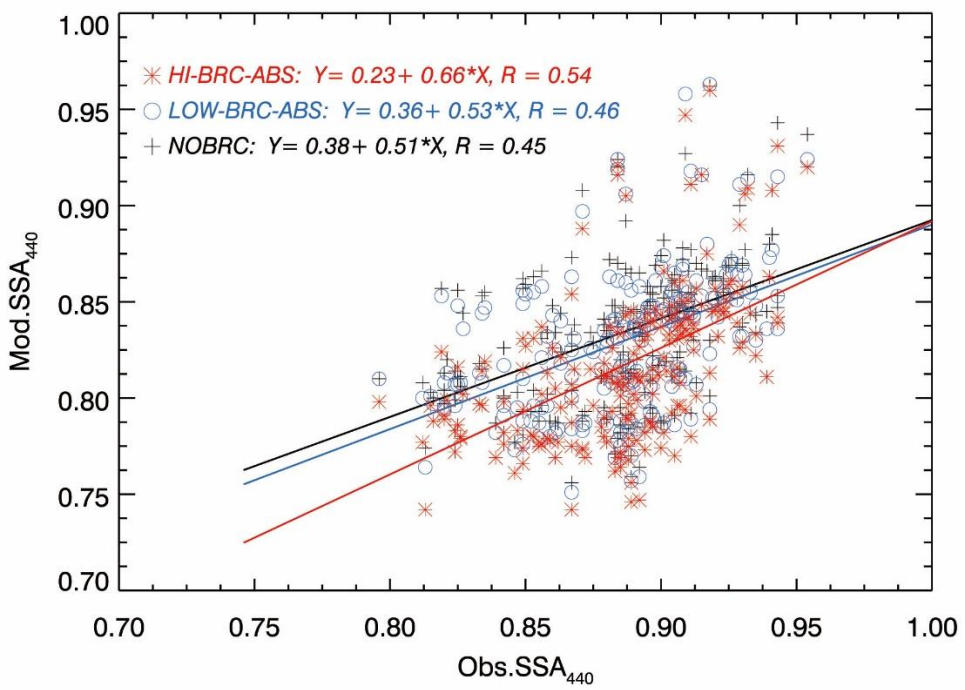

Figure 3. Scatter plot and linear fitting of modelled and observed column integrated SSA at 440 nm in the HI-BRC-ABS (red), LOW-BRC-ABS (blue) and NOBRC (black) case.

References

Cheng, Z., Atwi, K. M., Yu, Z., Avery, A., Fortner, E. C., Williams, L., Majluf, F., Krechmer, J. E., Lambe, A. T., and Saleh, R.: Evolution of the light-absorption properties of combustion brown carbon aerosols following reaction with nitrate radicals, Aerosol Science and Technology, 54, 849–863, https://doi.org/10.1080/02786826.2020.1726867, 2020.

D'Almeida, G.A., Koepke, P. and Shettle, E.P.: Atmospheric Aerosols: Global Climatology and Radiative Characteristics, A.Deepak Publ, Hampton, Virginia, 1991.

Dubovik, O., Holben, B., Eck, T. F., Smirnov, A., Kaufman, Y. J., King, M. D., Tanré, D., and Slutsker, I.: Variability of Absorption and Optical Properties of Key Aerosol Types Observed in Worldwide Locations, J. Atmos. Sci., 59, 590–608, https://doi.org/10.1175/1520-0469(2002)059<0590:VOAAOP>2.0.CO;2, 2002.

Feng, Y., Ramanathan, V., and Kotamarthi, V. R.: Brown carbon: A significant atmospheric absorber of solar radiation?, Atmos. Chem. Phys., 13, 8607–8621, 2013.

Forrister, H., Liu, J., Scheuer, E., Dibb, J., Ziemba, L., Thornhill, K. L., Anderson, B., Diskin, G., Perring, A. E., Schwarz, J. P., Campuzano-Jost, P., Day, D. A., Palm, B. B., Jimenez, J. L., Nenes, A., and Weber, R. J.: Evolution of brown carbon in wildfire plumes, Geophys. Res. Lett., 42, 4623–4630, https://doi.org/10.1002/2015GL063897, 2015.

Hurley, M. D., Sokolov, O., Wallington, T. J., Takekawa, H., Karasawa, M., Klotz, B., Barnes, I., and Becker, K. H.: Organic aerosol formation during the atmospheric degradation of toluene, Environmental science & technology, 35, 1358–1366, https://doi.org/10.1021/es0013733, 2001.

Jacobson, M. Z.: Isolating nitrated and aromatic aerosols and nitrated aromatic gases as sources of ultraviolet light absorption, J. Geophys. Res., 104, 3527–3542, https://doi.org/10.1029/1998JD100054, 1999.

Jeong, J. I., Jo, D. S., Park, R. J., Lee, H.-M., Curci, G., and Kim, S.-W.: Parametric analysis for global single scattering albedo calculations, Atmospheric Environment, 234, 117616, https://doi.org/10.1016/j.atmosenv.2020.117616, 2020.

Jo, D. S., Park, R. J., Lee, S., Kim, S.-W., and Zhang, X.: A global simulation of brown carbon: Implications for photochemistry and direct radiative effect, Atmos. Chem. Phys., 16, 3413–3432, https://doi.org/10.5194/acp-16-3413-2016, 2016.

Laskin, A., Laskin, J., and Nizkorodov, S. A.: Chemistry of atmospheric brown carbon, Chemical reviews, 115, 4335–4382, https://doi.org/10.1021/cr5006167, 2015.

Li, C., He, Q., Hettiyadura, A. P. S., Käfer, U., Shmul, G., Meidan, D., Zimmermann, R., Brown, S. S., George,

C., Laskin, A., and Rudich, Y.: Formation of Secondary Brown Carbon in Biomass Burning Aerosol Proxies through NO3 Radical Reactions, Environmental science & technology, 54, 1395–1405, https://doi.org/10.1021/acs.est.9b05641, 2020.

Li, G., Zavala, M., Lei, W., Tsimpidi, A. P., Karydis, V. A., Pandis, S. N., Canagaratna, M. R., and Molina, L. T.: Simulations of organic aerosol concentrations in Mexico City using the WRF-CHEM model during the MCMA-2006/MILAGRO campaign, Atmos. Chem. Phys., 11, 3789–3809, https://doi.org/10.5194/acp-11-3789-2011, 2011.

Lin, G., Penner, J. E., Flanner, M. G., Sillman, S., Xu, L., and Zhou, C.: Radiative forcing of organic aerosol in the atmosphere and on snow: Effects of SOA and brown carbon, J. Geophys. Res., 119, 7453–7476, https://doi.org/10.1002/2013JD021186, 2014.

Lin, P., Bluvshtein, N., Rudich, Y., Nizkorodov, S. A., Laskin, J., and Laskin, A.: Molecular Chemistry of Atmospheric Brown Carbon Inferred from a Nationwide Biomass Burning Event, Environmental science & technology, 51, 11561–11570, https://doi.org/10.1021/acs.est.7b02276, 2017.

Liu, D., Whitehead, J., Alfarra, M. R., Reyes-Villegas, E., Spracklen, D. V., Reddington, C. L., Kong, S., Williams, P. I., Ting, Y.-C., Haslett, S., Taylor, J. W., Flynn, M. J., Morgan, W. T., McFiggans, G., Coe, H., and Allan, J. D.: Black-carbon absorption enhancement in the atmosphere determined by particle mixing state, Nature Geosci, 10, 184–188, https://doi.org/10.1038/ngeo2901, 2017.

Moise, T., Flores, J. M., and Rudich, Y.: Optical properties of secondary organic aerosols and their changes by chemical processes, Chemical reviews, 115, 4400–4439, https://doi.org/10.1021/cr5005259, 2015.

Sun, J., Zhang, Y., Zhi, G., Hitzenberger, R., Jin, W., Chen, Y., Wang, L., Tian, C., Li, Z., Chen, R., Xiao, W., Cheng, Y., Yang, W., Yao, L., Cao, Y., Huang, D., Qiu, Y., Xu, J., Xia, X., Yang, X., Zhang, X., Zong, Z., Song, Y., and Wu, C.: Brown carbon's emission factors and optical characteristics in household biomass burning: Developing a novel algorithm for estimating the contribution of brown carbon, Atmos. Chem. Phys., 21, 2329–2341, https://doi.org/10.5194/acp-21-2329-2021, 2021.

Sun, J., Zhi, G., Hitzenberger, R., Chen, Y., Tian, C., Zhang, Y., Feng, Y., Cheng, M., Zhang, Y., Cai, J., Chen, F., Qiu, Y., Jiang, Z., Li, J., Zhang, G., and Mo, Y.: Emission factors and light absorption properties of brown carbon from household coal combustion in China, Atmos. Chem. Phys., 17, 4769–4780, https://doi.org/10.5194/acp-17-4769-2017, 2017.

Tuccella, P., Curci, G., Pitari, G., Lee, S., and Jo, D. S.: Direct Radiative Effect of Absorbing Aerosols: Sensitivity to Mixing State, Brown Carbon, and Soil Dust Refractive Index and Shape, J. Geophys. Res. Atmos., 125, 317, https://doi.org/10.1029/2019JD030967, 2020.

Turpin, B. J. and Lim, H.-J.: Species Contributions to PM2.5 Mass Concentrations: Revisiting Common Assumptions for Estimating Organic Mass, Aerosol Science and Technology, 35, 602–610, https://doi.org/10.1080/02786820152051454, 2001.

Wang, Q., Zhou, Y., Ma, N., Zhu, Y., Zhao, X., Zhu, S., Tao, J., Hong, J., Wu, W., Cheng, Y., and Su, H.: Review of Brown Carbon Aerosols in China: Pollution Level, Optical Properties, and Emissions, J. Geophys. Res., 127, 455, 2022.

Wang, X., Heald, C. L., Ridley, D. A., Schwarz, J. P., Spackman, J. R., Perring, A. E., Coe, H., Liu, D., and Clarke, A. D.: Exploiting simultaneous observational constraints on mass and absorption to estimate the global direct radiative forcing of black carbon and brown carbon, Atmos. Chem. Phys., 14, 10989–11010, https://doi.org/10.5194/acp-14-10989-2014, 2014.

Wang, X., Heald, C. L., Liu, J., Weber, R. J., Campuzano-Jost, P., Jimenez, J. L., Schwarz, J. P., and Perring, A. E.: Exploring the observational constraints on the simulation of brown carbon, Atmos. Chem. Phys., 18, 635–653, https://doi.org/10.5194/acp-18-635-2018, 2018.

Washenfelder, R. A., Attwood, A. R., Brock, C. A., Guo, H., Xu, L., Weber, R. J., Ng, N. L., Allen, H. M., Ayres, B. R., Baumann, K., Cohen, R. C., Draper, D. C., Duffey, K. C., Edgerton, E., Fry, J. L., Hu, W. W., Jimenez, J. L., Palm, B. B., Romer, P., Stone, E. A., Wooldridge, P. J., and Brown, S. S.: Biomass burning dominates brown carbon absorption in the rural southeastern United States, Geophys. Res. Lett., 42, 653–664, https://doi.org/10.1002/2014GL062444, 2015.

Wong, J. P. S., Tsagkaraki, M., Tsiodra, I., Mihalopoulos, N., Violaki, K., Kanakidou, M., Sciare, J., Nenes, A., and Weber, R. J.: Atmospheric evolution of molecular-weight-separated brown carbon from biomass burning, Atmos. Chem. Phys., 19, 7319–7334, https://doi.org/10.5194/acp-19-7319-2019, 2019.

Xu, L., Lin, G., Liu, X., Wu, C., Wu, Y., and Lou, S.: Constraining Light Absorption of Brown Carbon in China and Implications for Aerosol Direct Radiative Effect, Geophys. Res. Lett., 51, 455, https://doi.org/10.1029/2024GL109861, 2024.

Zhang, A., Wang, Y., Zhang, Y., Weber, R. J., Song, Y., Ke, Z., and Zou, Y.: Modeling the global radiative effect of brown carbon: A potentially larger heating source in the tropical free troposphere than black carbon, Atmos. Chem. Phys., 20, 1901–1920, https://doi.org/10.5194/acp-20-1901-2020, 2020.

Zhu, Y., Wang, Q., Yang, X., Yang, N., and Wang, X.: Modeling Investigation of Brown Carbon Aerosol and Its Light Absorption in China, Atmosphere, 12, 892, https://doi.org/10.3390/atmos12070892, 2021.